Limnol. Oceanogr., 57(6), 2012, 1634–1650

doi:10.4319/lo.2012.57.6.1634

Carbon mineralization and oxygen dynamics in sediments with deep oxygen penetration, Lake Superior

Jiying Li,[a] Sean A. Crowe,[b] David Miklesh,[c] Matthew Kistner,[a,c] Donald E. Canfield,[b] and Sergei Katsev [a,c,*]

[a] Large Lakes Observatory, University of Minnesota Duluth
[b] Nordic Center for Earth Evolution, University of Southern Denmark
[c] Department of Physics, University of Minnesota Duluth

Abstract

To understand carbon and oxygen dynamics in sediments with deep oxygen penetration, we investigated eight locations (160–318-m depth) throughout Lake Superior. Despite the 2–4 weight percent organic carbon content, oxygen penetrated into the sediment by 3.5 to > 12 cm at all locations. Such deep penetration is explained by low sedimentation rates (0.01–0.04 cm yr^{-1}), high solubility of oxygen in freshwater, and a shallow (~ 2 cm) bioturbation zone. In response mainly to oxygen variations in the bottom waters, the sediment oxygen penetration varied seasonally by as much as several centimeters, suggesting that temporal variability in deeply oxygenated sediments may be greater than previously acknowledged. The oxygen uptake rates (4.4–7.7 mmol m^{-2} d^{-1}, average 6.1 mmol m^{-2} d^{-1}) and carbon mineralization efficiency (~ 90% of deposited carbon) were similar to those in marine hemipelagic and pelagic sediments of comparable sedimentation rates. The reactivity of organic carbon was found to decrease with age similarly to the power-law documented in marine environments. The burial flux of carbon into the deep sediment (0.7 mmol m^{-2} d^{-1}) was 2.5% of the previously estimated primary production. Maximum volume-specific carbon degradation rates were 0.3–1.5 μmol cm^{-3} d^{-1}; bioturbation coefficient near the sediment surface was 3–8 cm^2 yr^{-1}. These results indicate that carbon cycling in large freshwater systems conforms to many of the same trends as in marine systems.

The sediments of lakes and reservoirs accumulate organic carbon (C) at a higher global annual rate than the ocean seafloor (Tranvik et al. 2009), yet their sediments remain understudied in terms of C burial, sequestration, and early diagenetic C remineralization (Cole et al. 2007; Gudasz et al. 2010). In comparison to marine environments, there is relatively little information on the rates and pathways of C degradation in lake sediments (Thomsen et al. 2004). In previous studies, carbon mineralization rates were shown to correlate with temperature (Gudasz et al. 2010) and oxygen exposure time (Sobek et al. 2009), but there have been few rigorous examinations of the relationships between C reactivity, burial efficiency, water depth, sedimentation rate, temperature, and electron acceptor availability (den Heyer and Kalff 1998; Sobek et al. 2009). Direct comparisons of freshwater environments with marine systems are complicated by a number of obvious differences in water column mixing rates and chemistry, notably the limited supply of sulfate in lakes, which through microbial sulfate reduction contributes to nearly 50% of the total carbon mineralization in marine sediments (Jørgensen 1982). Another principal difference is a lower biogeochemical reactivity of the terrigenous organic material that is brought into the lakes from the catchment and makes up a significant portion of the organic carbon pool in small and medium-sized lakes (Sobek et al. 2009). The largest lakes of the world, where organic matter is predominantly autochthonous, therefore, provide the best comparisons to marine systems (Johnson et al. 1982). In this study, we investigate the carbon mineralization processes in the sediments of Lake Superior, the world's largest freshwater lake by area, where terrigenous carbon inputs to the open lake do not exceed 17% of the total carbon budget (Zigah et al. 2011).

With its great depth, cold water, and low shoreline population density, Lake Superior has the lowest primary productivity of the Great Lakes (Munawar and Munawar 1978). Its sediments accumulate slowly (< 1 mm yr^{-1}) and have organic matter content below 5% (Johnson et al. 1982). The sediments are characterized by deep (> 4 cm) penetration of oxygen (Carlton et al. 1989), and thus oxygen is likely the dominant electron acceptor for organic carbon oxidation. Modeling studies (Katsev et al. 2006) have demonstrated that, in sediments with deep oxygen penetration, the oxygen penetration depth (OPD) may be sensitive to variations in the sedimentation flux of organic carbon and oxygen concentration in the water column. Changes in the OPD indicate shifts in the mineralization pathways of organic matter and likely coincide with strong modifications of sediment composition and rates of sediment–water material exchange. Seasonal shifts in sediment OPD by several centimeters or more have been observed in organic-poor deep-ocean environments (Sayles 1994; Gehlen et al. 1997), and have been postulated in others, such as the deep Arctic Ocean (Gobeil et al. 2001). By sampling Lake Superior sediments at multiple locations and in multiple seasons, we aim to constrain seasonal and geographical variability in oxygen dynamics.

The budget of organic carbon in Lake Superior remains poorly constrained and the putative long-term variation in

* Corresponding author: skatsev@d.umn.edu

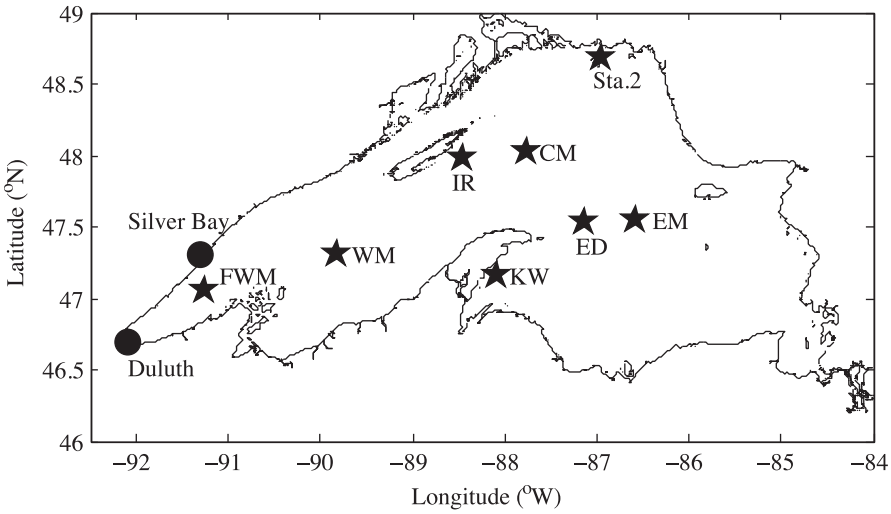

Fig. 1. Sampling locations in Lake Superior. Distances between substations (Table 1), are smaller than the size of the symbol.

primary productivity is poorly documented (Sterner 2010, 2011). Primary production, estimated at 9.7 Tg yr^{-1} (Sterner 2010), supplies most of the organic carbon to the water column (Ostrom et al. 1998), whereas riverine and atmospheric inputs account, respectively, for ~ 6% and 9% of the total organic carbon input to the lake (Cotner et al. 2004). Losses of organic carbon are primarily through water column respiration, estimates of which ranged between 13 and 39 Tg yr^{-1} (Cotner et al. 2004), making the carbon budget appear unbalanced, as losses exceed carbon inputs (Sterner 2010). The flux of organic carbon to sediments was estimated using sediment traps at 0.83 Tg yr^{-1} (Heinen and McManus 2004). The uncertainty in these estimates with respect to the total carbon budgets of the lake is large, mostly due to a geographical sampling bias, as most measurements have been made in the Western arm of the lake (McManus et al. 2003), where the primary production and terrestrial carbon inputs are thought to be higher. Data for the winter season are scant but suggest that winter production is not a negligible part of the annual carbon budget (Sterner 2010). Given the uncertainties and the inherent variability and patchiness in the water column measurements, sediment carbon degradation rates may provide a more robust estimate for the lake-average carbon sedimentation flux. Sediment studies also allow the determination of the efficiency of carbon retention in the sediment. In this study, we use the sediment distributions of organic carbon and the rates of oxygen consumption to characterize the sediment carbon cycle in Lake Superior, constrain its contributions to the lake-wide carbon budget, and compare the characteristics of this large freshwater system to the relationships established for marine sediments.

Methods

Sediment and water column samples were taken on several cruises aboard the R/V *Blue Heron* (Table 1; Fig. 1). Temperature and dissolved oxygen distributions in the water column were measured using a Seabird 911plus conductivity–temperature–depth probe with an Oxyguard flow-through oxygen sensor. Sediment cores of 94-mm inner diameter were recovered using an Ocean Instruments multi-corer. The landing sites were monitored using a Knudsen 320/R echo sounder with a 28-kHz transducer to

Table 1. Sampling dates and locations (Far Western [FWM], Eastern [EM], Western [WM], Isle Royale [IR], Central [CM], Eastern Deep [ED], Keweenaw [KW], and Slate Islands [Sta. 2]).

Date	Sta.	Depth (m)	Latitude (N)	Longitude (W)
03 Jun 2009	FWM.1	170	47 02.90	91 14.97
10 Nov 2009	FWM.2	160	47 06.26	91 43.19
07 Jun 2010	FWM.3	166	47 09.13	91 16.44
20 Jul 2010	FWM.4	168	47 02.14	91 16.38
21 Sep 2010	FWM.5	166	47 01.98	91 16.50
21 Apr 2011	FWM.6	166	47 02.15	91 16.31
05 Jun 2009	EM.1	218	47 32.54	86 34.31
06 Oct 2009	EM.2	225	47 32.52	86 34.31
10 Jun 2010	EM.3	229	47 33.38	86 35.76
22 Jul 2010	EM.4	228	47 33.36	86 35.65
22 Sep 2010	EM.5	226	47 33.37	86 35.68
04 Jun 2009	WM.1	175	47 18.32	89 49.43
04 Oct 2009	WM.2	170	47 18.29	89 49.73
11 Jun 2010	WM.3	169	47 19.01	89 50.73
22 Jul 2010	WM.4	174	47 18.26	89 49.33
25 Sep 2010	WM.5	169	47 19.05	89 50.76
23 Apr 2011	WM.6	171	47 19.01	89 50.80
08 Jun 2010	IR.1	234	47 58.41	88 28.01
21 Jul 2010	IR.2	237	47 58.42	88 28.07
22 Sep 2010	IR.3	235	47 58.41	88 28.08
21 Apr 2011	IR.4	235	47 58.40	88 27.97
08 Jun 2010	CM.1	252	48 01.06	87 46.44
21 Jul 2010	CM.2	236	48 02.84	87 47.32
22 Sep 2010	CM.3	235	48 02.66	87 47.17
22 Apr 2011	CM.4	239	48 03.04	87 47.74
21 Jul 2010	ED.1	316	47 31.81	87 07.81
22 Sep 2010	ED.2	318	47 31.53	87 07.49
22 Apr 2011	ED.3	312	47 31.76	87 07.65
09 Jun 2010	KW	84	47 09.85	88 05.32
04 Jun 2009	Sta. 2	100	48 41.0	86 57.2

select flat areas with laterally homogeneous sediment accumulation. The cores were subsequently stored at 4°C, which corresponds to the temperature (3–5°C) of Lake Superior bottom waters from May to November (*see* data below). Vertical distributions of dissolved oxygen in sediment pore waters were determined onboard in subsampled cores that were thermostated and allowed to equilibrate for about 40 min. Oxygen concentrations were measured using a Unisense (Clark-type) microelectrode (Revsbech 1989). The electrodes were calibrated at O_2 saturation in water at the in situ temperature (~ 4°C), and a buffered sodium ascorbate solution was used as a zero. On one cruise (October 2009), the electrodes were calibrated at 0% in water that was bubbled with nitrogen. Possible stagnation of the diffusive boundary layer during profiling is not expected to have significantly affected the oxygen gradients inside the sediment, as oxygen consumption was slow: profile shapes changed insignificantly over several hours. Rates of total oxygen uptake were measured during the June 2009 (in cores from Sta. FWM.1, WM.1, EM.1, and Sta. 2; Table 1) and September 2010 (Sta. FWM.5 and Sta. IR.3) cruises in 2–4 undisturbed intact sediment cores per each sampled site. To maximize the sensitivity of the measurements, these cores were collected with only 10–15 cm of overlying water. The cores were maintained at 4°C in the dark and the overlying water was stirred at 60 revolutions min^{-1} using a magnetic stir bar suspended 3–4 cm above the sediment–water interface. Oxygen concentrations were measured using Clark-type microelectrodes (Unisense) that were sealed into the tops of the core tubes with thick rubber stoppers. Oxygen concentrations decreased < 10% from their in situ values and the measured decrease was linear throughout the incubation period.

Separate sediment cores were sectioned onboard under an N_2 atmosphere at vertical intervals varying from 0.5 cm at the sediment surface to 5 cm below 20 cm. The organic carbon content was determined in freeze-dried sediment samples by coulometry on a CM150 total carbon, total organic carbon (TOC), total inorganic carbon analyzer. Sediment water content was determined by comparing the sediment sample weights before and after freeze-drying. Porosity was calculated as $\varphi = (M_w/\rho_{H2O})/[(M_d/\rho) + (M_w/\rho_{H2O})]$, where M_w and M_d are, respectively, the weights of interstitial water and dry sediment, ρ_{H2O} is the density of water (1.00 g cm^{-3}), and ρ is the density of dry sediment (2.65 g cm^{-3}) (Johnson et al. 1982). Separate intact sediment cores were split, photographed, and analyzed on a Geotek multisensor core logger at the LacCore facility of the University of Minnesota. Sediment dating using ^{210}Pb was performed by the Flett Research Laboratory at the University of Manitoba on cores from Sta. EM and Sta. CM and by St. Croix laboratory of the Science Museum of Minnesota on cores from Sta. IR and Sta. FWM. The sediment age and accumulation rates (g cm^{-2} yr^{-1}) were determined by the analyzing laboratories using a constant rate of supply (CRS) model (Appleby and Oldfield 1978) and measured dry mass per volume of wet sediment. Burial velocities U (cm yr^{-1}) were calculated from the obtained age-vs.-depth relationships as a function of depth x as

$$U = \frac{dx}{dt} \tag{1}$$

The CRS model likely overestimates slightly the sedimentation rates within the bioturbation zone; however, in Lake Superior only the upper 2 cm of sediment are bioturbated (*see* below).

Calculation of oxygen fluxes, bioturbation rates, carbon mineralization rates, and carbon reactivity—The diagenesis of solutes and solid phases can be described with a set of diagenetic equations (Berner 1980). If x is the depth below the sediment–water interface and $C_i(x,t)$ is the concentration of a chemical species i in solid phase (in mol per dry weight) or pore water (in mol per pore-water volume), then for solutes (Katsev et al. 2007):

$$\frac{\partial \varphi C_i}{\partial t} = \frac{\partial}{\partial}\left(\varphi D_i \frac{\partial C}{\partial x}\right) - \frac{\partial}{\partial x}(\varphi U C_i) + \varphi \alpha_{irr}\left(C_i^0 - C_i^{burr}\right) + \sum_j R_j \tag{2}$$

and for solid phases:

$$\frac{\partial \xi C_i}{\partial t} = \frac{\partial}{\partial}\left(\xi D_b \frac{\partial C}{\partial x}\right) - \frac{\partial}{\partial x}(\xi U C_i) + \sum_j R_{ij} \tag{3}$$

Here, D_i is the effective diffusion coefficient, U is the advection (burial) velocity, R_{ij} are the rates (mol per volume of bulk sediment) of all reactions that affect the species i, φ is the porosity, and the factor ξ is equal to $(1 - \varphi)\rho$, where ρ is the density of dry sediment. The coefficient α_{irr} describes bioirrigation, which is a fauna-mediated, nonlocal (non-diffusive) exchange of fluids between the sediment surface (concentration C_i^0) and bioirrigated burrows (C_i^{burr}). The diffusion of solid particles is due to bioturbation (Berner 1980; Meysman et al. 2005), described by the bioturbation coefficient, D_b. When temporal changes in the sediment are slow, so that the species distributions approach a dynamic equilibrium, a quasi–steady state can be described by setting the left-hand side of these equations to zero.

For oxygen in non-permeable sediments, diffusion typically dominates over advection, so the advection term in Eq. 2 can be neglected. The bioirrigation term is an important component of oxygen fluxes in marine sediments, although in freshwater sediments it is sometimes claimed to be insignificant (Sweerts et al. 1991). Given the lack of data on bioirrigation in Lake Superior, we do not include it in the calculation of oxygen fluxes, with a caveat that the actual oxygen fluxes may be higher than calculated. To estimate the maximum potential contribution from bioirrigation, we compare the calculated diffusive oxygen fluxes with the total oxygen uptakes determined in core incubations. The diffusive fluxes of oxygen, F_{O_2} (mol m^{-2} d^{-1}), within the sediment can be calculated using the Fick's law of diffusion:

$$F_{O_2} = -\varphi(D_s + D_{ehn})\frac{d[O_2]}{dx} \tag{4}$$

Table 2. Diffusive oxygen fluxes are the maximum values averaged over all available profiles for the given station. Numbers in brackets give the minimum and maximum values for the station. The total oxygen uptake values are from whole-core incubations. Maximum carbon degradation rates are equivalent to the maximum oxygen consumption rates (e.g., Fig. 4), averaged over all available profiles.

Station	Diffusive flux (mmol m^{-2} d^{-1})	Total uptake (mmol m^{-2} d^{-1})	Maximum carbon mineralization rate (R_C) (μmol cm^{-3} d^{-1})	Organic carbon reactivity at SWI, k (yr^{-1})	Mineralization time scale, τ (yr)
FWM	3.04(1.04–7.80)	6.37; 7.1±1.1	0.60(0.11–2.18)	1.34	0.52
WM	2.20(1.05–3.20)	4.44	0.47(0.15–0.98)		
EM	2.27(1.34–4.59)	8.29*	0.52(0.30–1.13)	1.33	0.52
IR	4.98(2.72–7.27)	4.9±0.8	1.39(0.83–1.51)	2.62	0.26
CM	3.16(2.30–3.77)		0.70(0.49–1.05)	0.78	0.89
ED	4.15(2.73–6.75)		0.89(0.59–1.38)	0.74	0.94
KW	2.89		0.29		
Sta. 2	4.08	7.68	0.83		
Average	3.02±1.50	6.10±1.39	0.64	1.36±0.76	0.63

Here, the diffusion coefficient, $D_s = D/\theta^2$, is the molecular diffusion coefficient of oxygen, D = 421 cm^2 yr^{-1} (at T = 4°C; Boudreau 1997), corrected for sediment porosity φ using the tortuosity factor, $\theta^2 = 1 - \ln(\varphi^2)$ (Boudreau 1997). The diffusion-like transport of oxygen by benthic fauna is characterized by the enhanced diffusion coefficient, D_{enh} (Meile and Van Cappellen 2003). As the magnitude and depth dependence of D_{enh} are not known a priori, we adopt the same approach as for the nonlocal bioirrigation coefficient, α_{irr}: we disregard it in the calculations but estimate its contribution later by comparing the calculated diffusive fluxes with the fluxes measured in incubations. Using Eq. 4, the diffusive fluxes of oxygen within the sediment were therefore calculated from high-resolution oxygen microelectrode profiles and sediment porosity (Sauter et al. 2001) as

$$F_{O_2} \approx -\varphi D_s \frac{d[O_2]}{dx} \tag{5}$$

To estimate the transport of particulate organic carbon by bioturbation, we use Eq. 3, building on the approach of Canfield et al. (1993) and Thomsen et al. (2004). For organic carbon, the (negative) reaction term ΣR_j represents the total rate of organic carbon mineralization, R_C. At a quasi–steady state, the partial derivatives with respect to x in Eq. 3 can be replaced by ordinary derivatives. By integrating Eq. 3 from some depth L within the sediment to x, we obtain:

$$\xi_x D_b \left(\frac{dC}{dx}\right)_x - (\xi_x U_x C_x - \xi_L U_L C_L) - \int_L^x R_C(x')dx' = 0 \tag{6}$$

Here, we choose L sufficiently deep into the sediment so that $D_b(x = L) = 0$. We also use the minus sign in front of the reaction term R_C to explicitly indicate that it results in consumption of organic carbon. The integral in Eq. 6 represents the total rate of organic carbon mineralization below the depth x. As oxygen is used to oxidize both organic carbon and products of anaerobic metabolisms (*see* below), within the oxic zone this integral can be approximated by the downward flux of oxygen at depth x. By substituting the expression for F_{O_2} from Eq. 5 into Eq. 6, we obtain the bioturbation coefficient within the oxic zone as

$$D_b = \frac{(\xi_x U_x C_x - \xi_L U_L C_L) - \varphi D_s \left(\frac{d[O_2]}{dx}\right)_x}{\xi_x \left(\frac{dC}{dx}\right)_x} \tag{7}$$

For the calculations in this paper, the sediment accumulation rate, $\xi_L U_L$, and the organic carbon concentration, C_L, were evaluated at the bottom of sediment cores. The oxygen gradients were taken from the measured microprofiles, and the organic carbon concentrations and gradients were taken from the profiles determined by coulometry. As actual oxygen fluxes may be higher than molecular diffusion fluxes because of the bioirrigation and fauna-enhanced diffusion, the actual values of D_b may be correspondingly higher than calculated. Where sediment accumulation rate (g cm^{-2} yr^{-1}) can be considered approximately steady, a further simplification of Eq. 7 is possible, as $\xi_x U_x = \xi_L U_L$ (Meysman et al. 2005; Katsev et al. 2007).

The oxygen consumption rates per volume of sediment, R_{O_2}, were calculated assuming that the oxygen distributions were close to being in steady state, in which case oxygen consumption accounts for all changes in the vertical oxygen fluxes:

$$\frac{\partial \varphi [O_2]}{\partial t} = -\frac{\partial F_{O_2}}{\partial x} + R_{O_2} = 0 \tag{8}$$

Accordingly, the rates R_{O_2} (mol m^{-3} d^{-1}) (per volume of bulk sediment) were calculated by taking a derivative of the oxygen flux profile (Sauter et al. 2001):

$$R_{O_2} = -\frac{dF_{O_2}}{dx} \tag{9}$$

These profiles were smoothed by taking sliding averages with a typical window size of 2–4 mm. Again, within the bioturbation zone, the actual oxygen consumption rates may be higher than calculated due to the benthic fauna contribution to oxygen fluxes.

For carbon degradation rates limited by carbon availability (rather than by the availability of oxidants), the mineralization rate can be written as $R_C = k\xi C$, where C is

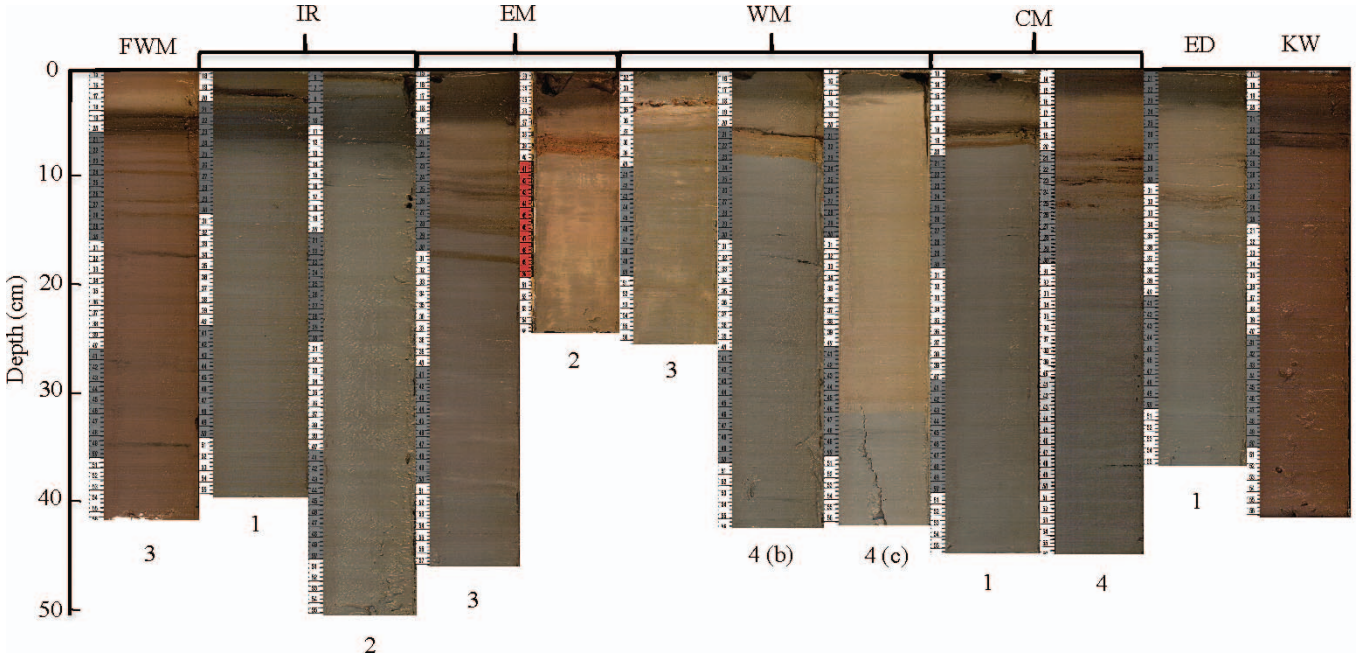

Fig. 2. Optical images of Lake Superior sediment cores. Note the strong variability in color and the presence of multiple metal layers that appear as distinct horizontal layers. The horizontal line indicates the positions of sediment–water interfaces. Numbers under the images indicate substations within each sampling station (Table 1). The vertical scale is the same for all cores.

the molar concentration (mol g^{-1}) of organic carbon. The first-order rate parameter k (yr^{-1}) is the effective reactivity of organic matter. As sediment organic matter consists of a large number of fractions that degrade at different rates, the effective reactivity decreases with sediment depth, as organic material ages and becomes depleted in labile fractions. Using the oxygen consumption rates, R_{O_2} (Eq. 9), as an approximation for the carbon degradation rates (R_C), we calculate the organic carbon reactivity (k), within the oxic zone as

$$k = R_{O_2}/(\xi C) \tag{10}$$

The characteristic half-life of organic C in the sediment is calculated as $\tau = \ln(2)/k$ (Table 2).

Results

Geographic variability in sediment properties—Sediments in Lake Superior exhibit strong lateral variability in their visual appearance, as well as vertical positions of characteristic diagenetic layers (Fig. 2). Sediments from nearshore locations (Sta. FWM, and Sta. KW) were predominantly brown, whereas gray clays dominated at the offshore locations. Most sediment cores showed prominent manganese (Mn)- and iron (Fe)-rich layers (Li 2011) between 4- and 14-cm depth below the sediment–water interface. The layers, whose compositions were verified using scanning X-ray fluorescence (Li 2011), were visible to the naked eye as rust-colored layers for Fe and black layers for Mn. Strikingly, some cores recovered within short distances to each other (Table 1) in deep Eastern (Sta. EM) and deep Western (Sta. WM) basins were markedly different in color and the number of metal-rich layers (Fig. 2). Variability in cores from other stations was smaller, but still significant, with the depths of metal-rich layers varying by up to several centimeters (Fig. 2).

Sediment accumulation rates—Sediment accumulation rates (g cm^{-2} yr^{-1}) determined from ^{210}Pb analyses are shown in Fig. 3. At Sta. FWM, the data show a temporary increase in sedimentation by more than a factor of 2 in the mid-20th century. This is likely associated with the discharge of taconite tailings (depleted iron ore) into the lake by the Silver Bay Mining Company (Fig. 1). The discharges continued from 1950s to 1980s and led to a markedly increased sedimentation in parts of the Western Arm of Lake Superior (Li 2011). Another contributing factor may be the variations in the amount of coarse-grained sediment carried into the lake by the St. Louis River, at the westernmost end of the lake. At other stations, sediment accumulation varied throughout the 20th century to a much smaller degree. Among these stations, Sta. IR has the highest sediment accumulation rate, around 0.02 g cm^{-2} yr^{-1}. The sites Sta. CM and Sta. EM, located, respectively, in the central and east-central parts of the lake, have significantly lower sedimentation rates, around 0.01 g cm^{-2} yr^{-1}. The burial velocities (cm yr^{-1}), which are the solid particle velocities relative to the sediment–water interface, decrease downcore due to sediment compaction, from $\sim$ 0.1 cm yr^{-1} near the sediment–water interface to 0.02–0.03 cm yr^{-1} below 10-cm depth.

Water column temperature and oxygen distributions—Temperature profiles in the water column (Fig. 4) at all stations indicated typical dimictic stratification, with spring overturn in early June and winter overturn known to occur in December. Temperatures in the bottom waters remained

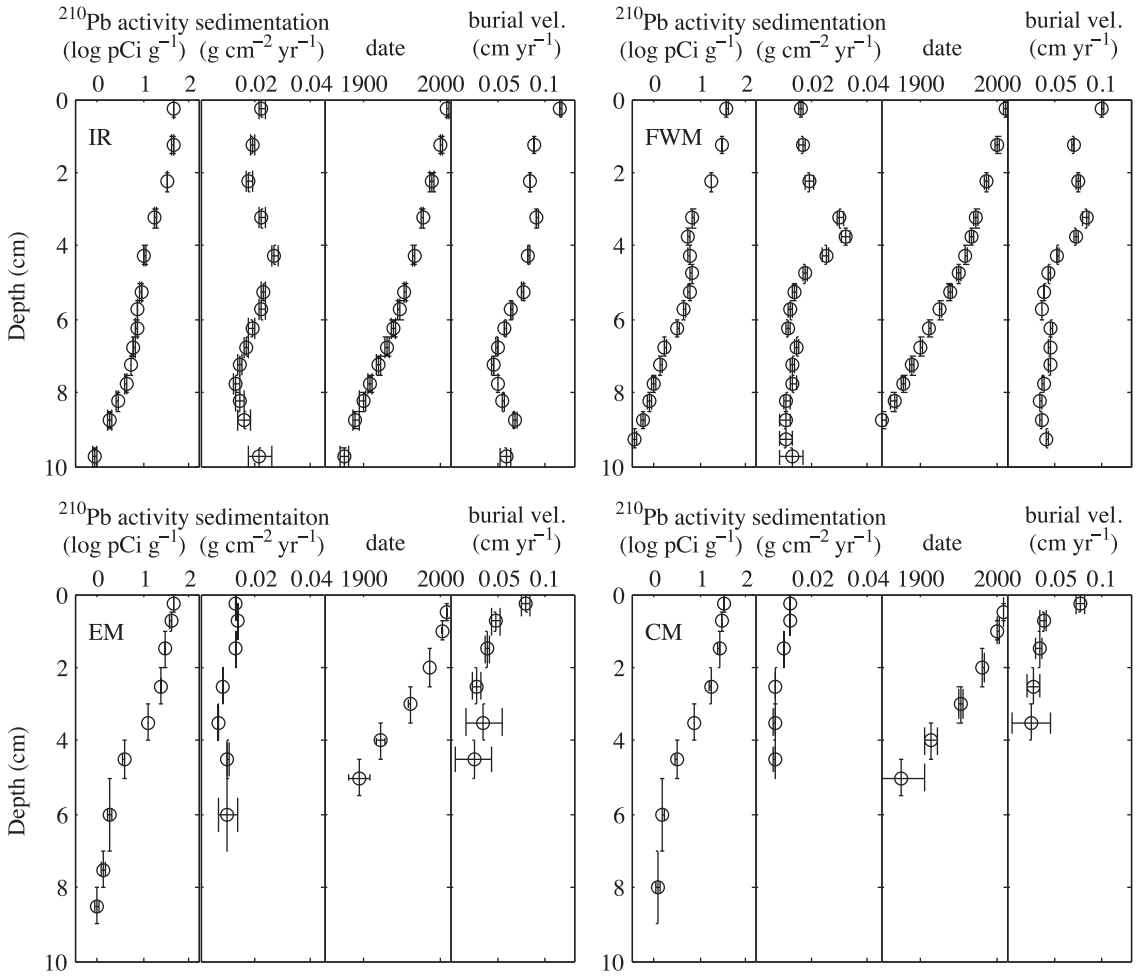

Fig. 3. Unsupported ^{210}Pb activity and the calculated sediment accumulation rates, apparent sediment ages, and burial velocities (vel.) at Sta. IR, FWM, EM, and CM. Horizontal error bars reflect the propagated uncertainties in the ^{210}Pb activity. Vertical error bars indicate the depth intervals of analyzed samples.

near the maximum-density temperature (4°C) year-round, with surface temperatures varying between 0°C in winter and 17°C in summer. Oxygen concentrations in the bottom waters were high after the overturn in June (near 400 μmol L^{-1}) and remained high (85% to 100% saturation) in early and midsummer but declined (to 250–300 μmol L^{-1}) in fall (Fig. 4). The oxygen dynamics during winter months are poorly known. Depth variation in oxygen within the epilimnion typically mirrored the temperature profiles, suggesting their control by oxygen solubility: lower concentrations were found in warmer surface waters during summer stratification.

Oxygen penetration and uptake—Oxygen penetrated deeply into the sediments at all locations (Fig. 5). The OPD, defined at the detection limit of the microelectrode (0.5 μmol L^{-1}), was between 4 and 11 cm in cores from Sta. FWM, CM, ED, and KW and several cores from Sta. WM and Sta. EM. In several other cores from Sta. WM and Sta. EM (EM.1, EM.2, WM.1, WM.2, WM.3, WM.4c), oxygen concentrations remained high ($>$ 80 μmol L^{-1}) to depths $>$ 12 cm, the maximum depth that could be reached with our microelectrode. Sediments in these cores were predominantly yellow (e.g., Sta. WM.4c in Fig. 2) and in some cores the sediment appeared horizontally heterogeneous, with pockets of different color within the same sediment layer (e.g., Sta. EM.2 and Sta. WM.3 in Fig. 2). At stations where sediment cores from different samplings were similar in appearance (Sta. IR, CM, ED, selected cores from Sta. EM), the depth of oxygen penetration varied between samplings throughout summer 2010 by several millimeters. Oxygen penetration typically deepened from June and July to September, especially at the sites with deep OPDs (Sta. EM and CM; Fig. 5). With the exception of Sta. CM, the oxygen penetration in April 2011 was significantly shallower (by $\sim$ 2 cm) at all sampled locations (Fig. 5). In comparison, replicate profiles taken in different cores of similar visual appearance from the same station during the same cruise differed in their OPDs by $<$ 2 mm.

Sediment oxygen uptake fluxes measured in core incubations varied between 4.4 mmol m^{-2} d^{-1} at Sta. WM to 7.7 mmol m^{-2} d^{-1} at Sta. 2, with an average of 6.1 mmol m^{-2} d^{-1} (Table 2). A higher value of 8.3 mmol m^{-2} d^{-1} was obtained in a single core at Sta. EM, but the incubation

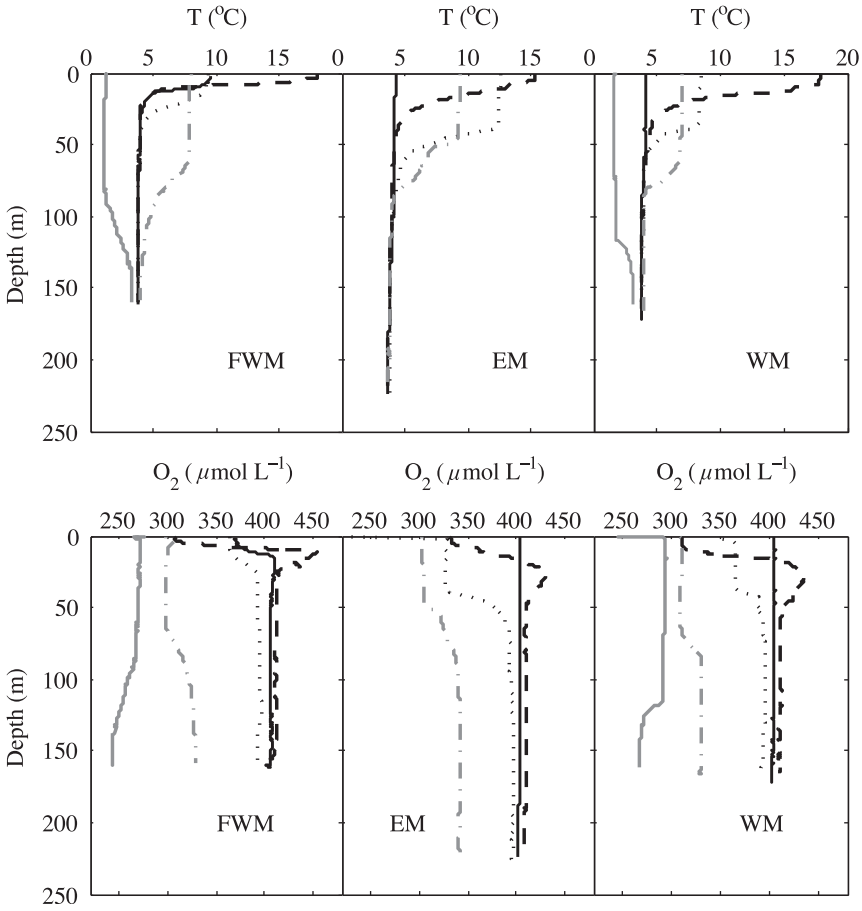

Fig. 4. Vertical distributions of temperature and dissolved oxygen in the water column of Lake Superior. The profiles illustrate seasonal variability between April (gray solid), June (dark solid), July (dark dashed), September (dark dot), and October and November (gray dash-dot). April profiles were from 2011; June, July, and September profiles were from 2010; October–November profiles were from 2009.

appeared disturbed, with sediment resuspension during core recovery. Figure 6 presents the diffusive oxygen fluxes, which were calculated from representative microelectrode oxygen profiles (Fig. 5). The calculated diffusive fluxes were consistently below the fluxes in incubations (Table 2), with the average diffusive flux being approximately half the average flux in incubations. At Sta. IR, where sediment composition appeared to be most consistent between samplings, the diffusive flux (3.29 mmol m^{-2} d^{-1}) in September 2010 was 67% of the total uptake flux (4.9 ± 0.8 mmol m^{-2} d^{-1}) measured on the same cruise. The calculated rates of oxygen consumption (Fig. 6) are highest within the top 1 cm of the sediment, with typical maximum values between 0.4 and 1.4 μmol cm^{-3} d^{-1} (Fig. 6; Table 2). The rates monotonously decrease downcore, with the exception of Sta. IR where the depth of oxygen penetration was shallowest among our locations and oxygen consumption had an apparent peak at around the OPD (e.g., in Sta. IR.1 core, oxygen consumption increased from 0.03 μmol cm^{-3} d^{-1} at 3.4 cm to 0.14 μmol cm^{-3} d^{-1} at 3.5 cm; Fig. 6). Figure 7 plots the calculated uptake fluxes, maximum volume-specific oxygen consumption rates, and oxygen concentrations in the bottom waters (Fig. 4) as a function of time of the year.

Organic carbon content and reactivity—The organic carbon content of the sediments decreases downcore from 3.5 to 5.0 weight percent (wt%) at the sediment surface to about 2 wt% in the deeper sediment (Fig. 8). The concentration of organic carbon remains relatively constant below 10–15-cm depth. At Sta. FWM, both the organic carbon concentration and water content varied non-monotonously (Fig. 8). The dip in the Sta. FWM profile at 4-cm depth indicates the presence of dense organic-poor particles, which matches the period of increased sedimentation (Fig. 3) and the time period during which taconite tailings were being discharged from Silver Bay (Li 2011).

The depth variation in the effective reactivity of organic carbon calculated from Eq. 10 is illustrated in Fig. 9. The calculations used the oxygen consumption rates from Fig. 6 and the organic carbon concentration (C) interpolated from the profiles in Fig. 8. The reactivity of organic carbon decreases drastically within the upper 1 cm of the sediment.

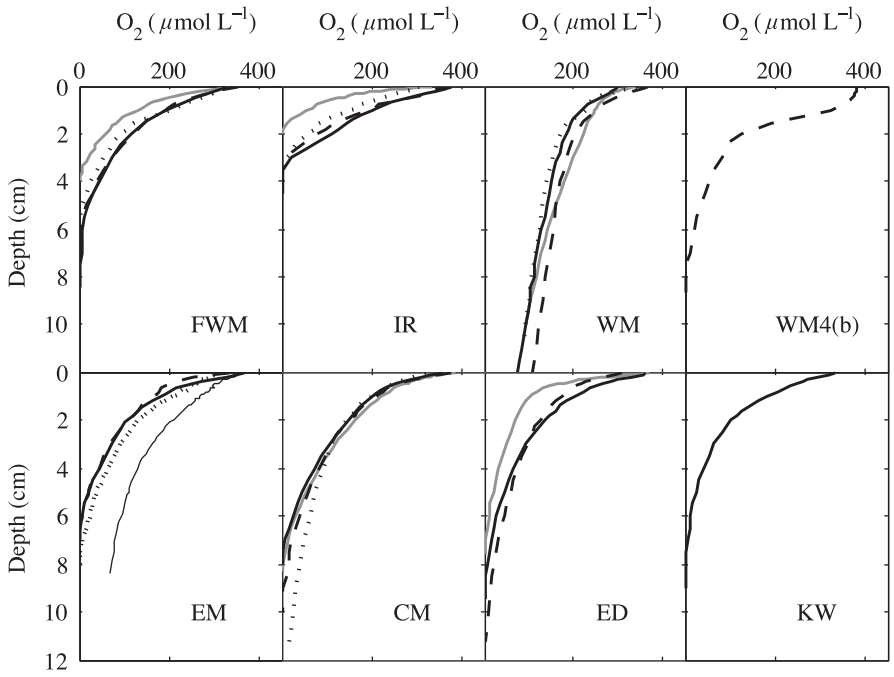

Fig. 5. Vertical distributions of dissolved oxygen in sediment pore waters in June (black solid), July (black dashed), and September (black dotted) of 2010 and April 2011 (gray solid). The thin solid line indicates a profile with deep OPD at Sta. EM.2 (October 2009) that was measured in a core whose appearance differed from other cores from that station (Fig. 2).

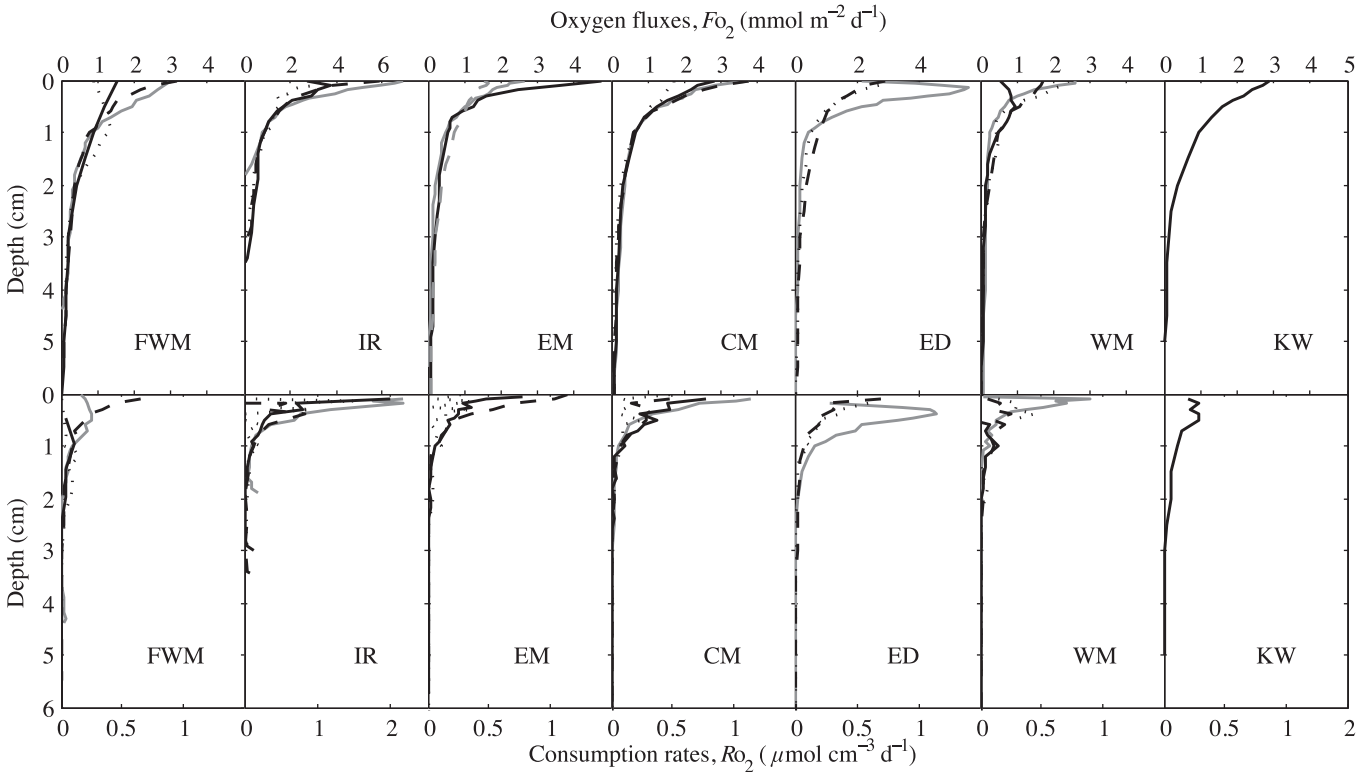

Fig. 6. Calculated oxygen fluxes (top) and consumption rates (bottom) in June (black solid), July (black dashed), and September (black dotted) of 2010 and April 2011 (gray solid).

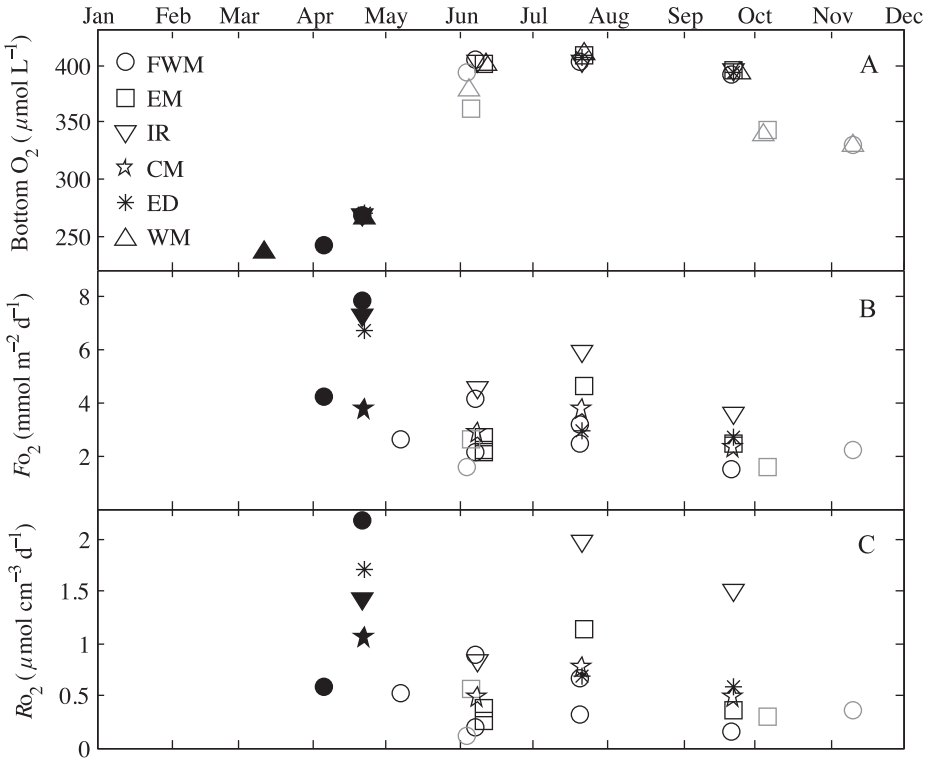

Fig. 7. (A) Seasonality in bottom-water oxygen concentrations determined from conductivity–temperature–depth data, (B) maximum sediment oxygen fluxes (F_{O_2}), and (C) maximum oxygen consumption rates (R_{O_2}). Black open symbols are the results from 2010; gray open symbols are from 2009; black solid symbols are the results from 2011.

At the sediment–water interface the reactivity k is around 1 yr^{-1}, whereas in the depth interval 1–2 cm it falls to $\sim$ 0.05 yr^{-1}.

Bioturbation rates—Figure 10 shows the values of the bioturbation coefficient calculated from Eq. 7, as a function of depth within the sediment. Bioturbation is limited to the upper 2 cm of sediment, consistent with our visual observations: below that depth, the sediment often contains distinct compositional layers (Fig. 2), which suggests the absence of mixing. Bioturbation is most intense at the sediment surface, where the bioturbation coefficient reaches values of 3–4 cm^2 yr^{-1}.

Discussion

Spatial variability—Our results reveal strong lateral variability in Lake Superior sediment properties, not only between sampling stations located hundreds of kilometers apart, but also over hundreds of meters. On large geographical scales, variability can be expected due to differences in sediment provenance, organic matter fluxes, and bottom current velocities. The Western basin, for example, has generally higher phytoplankton abundance (Munawar and Munawar 1978) and higher sediment burial rates (previously reported to be $\sim$ 0.04 cm yr^{-1} around Sta. FWM and 0.03 cm yr^{-1} around Sta. WM) than the Eastern basin ($\sim$ 0.01–0.03 cm yr^{-1} around Sta. EM) (Kemp et al. 1978; Evans et al. 1981). This could result in a shallower oxygen penetration in the Western basin. On a much smaller scale, however, our Sta. EM.1 core had no visible Fe-rich layer (Li 2011) and an OPD $>$ 12 cm, whereas our Sta. EM.2 core had a prominent Fe layer at 6-cm depth (Figs. 2, 5) yet an OPD $>$ 8 cm. Another core from the same site, Sta. EM.3, had an Fe-rich layer at $\sim$ 8.5 cm and an OPD of 6.5 cm (Figs. 2, 5). These cores were recovered within several hundred meters of each other. Such small-scale variability was strongest at the Sta. WM and Sta. EM stations, in the middle of the Western and Eastern deep basins, respectively. The strong variability in sediment properties in our cores may be linked to the spatial heterogeneity of the Lake Superior floor that was reported in recent seismic surveys (van Alstine 2006). The surveys, which focused on areas close to our Sta. WM, revealed that the lake floor contains multiple pockmarks, as well as linear and ring-shaped depressions that were $\sim$ 2 m deep and spanned hundreds of meters. Sediment core analyses suggested that the depressions expose the hard-packed postglacial sediments that may contain little recently deposited material (van Alstine 2006). The origin of these features is unclear; they have been hypothesized to be expressions of glacial ice scouring and dewatering of postglacial sediments (T. Johnson and N. Wattrus pers. comm.). Our observations with a shipboard echosounder indicate that these features are ubiquitous in both the Eastern and Western basins of the lake. Despite the strong

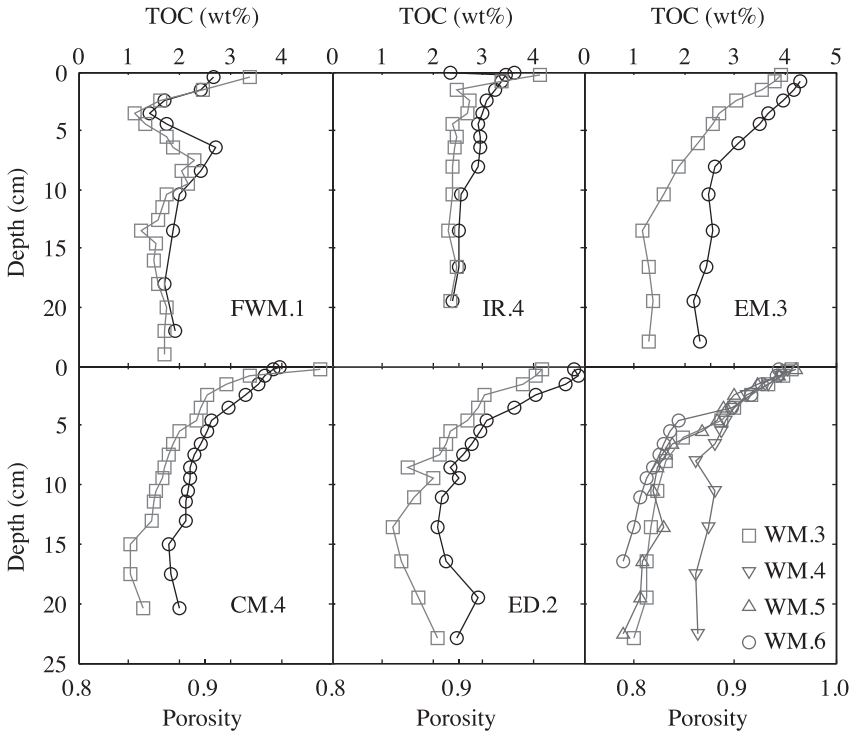

Fig. 8. Organic carbon (OC) content (black) and porosity (gray). The total inorganic carbon content (TIC) was negligible (< 0.1%) in all coulometric measurements. The non-monotonous decrease in OC content at the Sta. FWM is explained by the deposition of taconite tailings discharged into the lake from Silver Bay between 1955 and 1980.

spatial variability in sediment properties, the fluxes of dissolved oxygen across the sediment–water interface and several other geochemical features were relatively similar among our locations (Table 2).

Oxygen fluxes and consumption rates—The rate of total oxygen uptake by the sediment can be taken to represent the total rate of carbon degradation (R_C in Table 2), as oxygen is consumed through both aerobic respiration and oxidation of the reduced products of anaerobic metabolisms. An exception is the organic matter degraded through denitrification, as the N_2 produced is inert and not reoxidized within the sediment. Denitrification, however, is typically only a few percent of the total organic matter degradation (Canfield et al. 1993; Thomsen et al. 2004). In Lake Superior, where bottom-water nitrate concentrations are about 25–30 μmol L^{-1} (Sterner et al. 2007), its contribution was previously estimated to be < 5% (Li 2011). The possible oxidation of the reduced products of anaerobic metabolisms by nitrate, rather than oxygen, is reflected in the oxygen uptake through the in-sediment oxidation of ammonium, which exhibits insignificant fluxes across the sediment–water interface (Li 2011).

The total oxygen uptake rates (Table 2) measured in our incubations were greater than oxygen fluxes driven by molecular diffusion, suggesting a non-negligible contribution from processes such as fauna-enhanced diffusion, nonlocal bioirrigation, or hydrodynamic flow (Lorke et al. 2003; Glud 2008). The observed differences suggest that these processes may account for 30–50% of the total oxygen flux. This is at the low end of the range for the contribution of biologically enhanced fluxes in marine sediments with similar total oxygen uptakes (Meile and Van Cappellen 2003). For nonlocal bioirrigation, using the typical rates ($\alpha_{irr}C_0$ = 10–20 mmol L^{-1} yr^{-1}) in marine sediments (Meile and Van Cappellen 2003), and integrating the bioirrigation rate over 2 cm (the depth interval affected by benthic fauna in Lake Superior, Fig. 10), we calculate that the nonlocal bioirrigation flux of oxygen in Lake Superior is about 0.3 mmol m^{-2} d^{-1}. This is < 10% of the total uptake flux. A similarly small figure is obtained when the bioirrigation rates are calculated using the bioirrigation coefficients that were measured in microcosm experiments in Lake Erie sediments ($\alpha_{irr} = 10^{-6}$ s^{-1}; Matisoff and Wang 1998). This suggests that in Lake Superior the benthic fauna contributes to the solute transport primarily through enhanced diffusion, rather than nonlocal fluid exchange. Given the magnitude of this contribution (30–50% of the total uptake flux), the calculated rates of organic carbon decomposition (Fig. 6) and values of bioturbation coefficient (Fig. 10) likely underestimate the rates and coefficients by 30–50%.

Whereas the rates of oxygen consumption (R_{O_2}) in Fig. 6 were calculated (Eq. 9) with the assumption of a steady state, the data in Fig. 7 allow us to quantify the contribution of the time-explicit term in Eq. 8. The

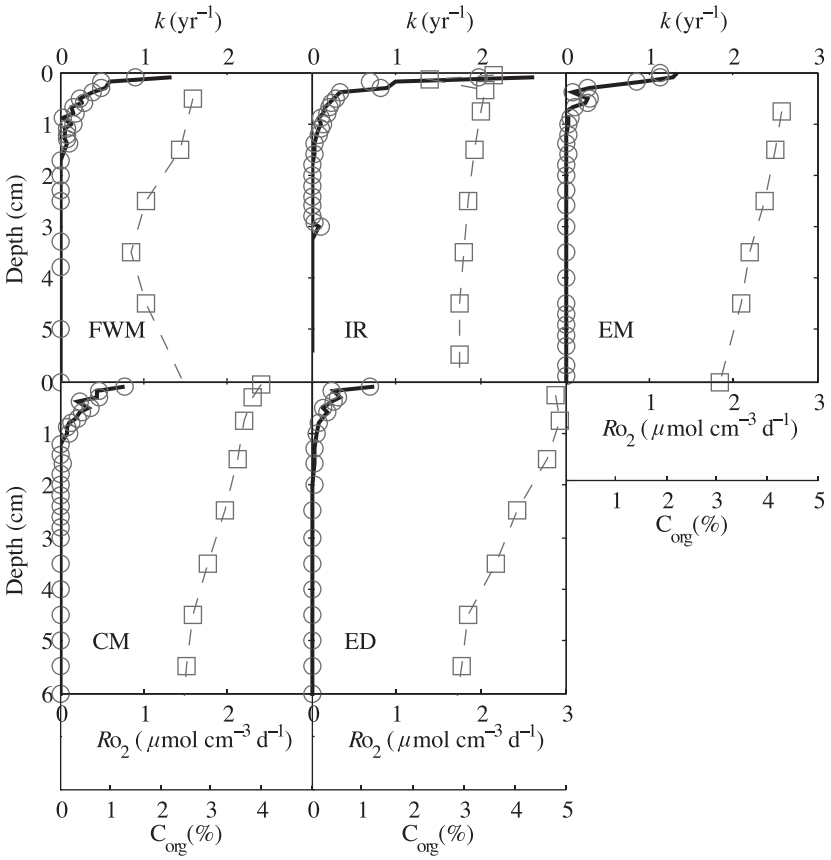

Fig. 9. Reactivity k (black line) of organic carbon, calculated from the rate of oxygen consumption $R_C = R_{O_2}$ (gray circles) and the concentration of total organic carbon (TOC, gray squares). The TOC profile was interpolated between measurements as shown by the dashed line.

fastest change in the bottom-water oxygen concentrations seems to have occurred in April–May, when the concentrations increased from 8 mg L^{-1} (250 μmol L^{-1}) to 13 mg L^{-1} (400 μmol L^{-1}) over a period of $\sim$ 60 d. This translates into the rate of change at the sediment–water interface of $\partial[O_2]/\partial t = 0.0025$ μmol cm^{-3} d^{-1}, which is two orders of magnitude lower than the typical rate of oxygen consumption (Fig. 7). As temporal variations below the sediment surface are expected to be even lower, the steady-state approximation given by Eq. 9 should be sufficiently precise. As R_{O_2} is representative of the rate of organic carbon degradation (R_C), Fig. 6 illustrates that the rates of organic carbon degradation in Lake Superior are highest near the sediment–water interface and decrease substantially within the upper 1–2 cm of sediment. A significant fraction of organic carbon is thus mineralized in the upper sediment layer, where oxygen, which penetrates well below the bioturbation zone, is present at high concentrations. Only profiles from Sta. IR indicate a substantial consumption of oxygen by the products of anaerobic metabolisms, as reflected by a local maximum in oxygen consumption at the oxic–anoxic boundary, which corresponds with the accumulation of Mn and Fe (oxyhydr)oxides (Li 2011) and likely develops due to the oxidation of upward diffusing reduced chemical constituents by O_2 (Canfield et al. 1993).

Carbon fluxes and reactivity—The rate of carbon burial into the deep sediment, $F_{C_{bur}}$, can be estimated from the sediment accumulation rate, $U\xi$, and the total organic carbon concentration (C), at a depth L where the concentration of organic carbon no longer varies appreciably with depth: $F_{C_{bur}} = C_L U_L \xi_L$. The sediments below 15-cm depth contain about 2% TOC (1.7 mmol C g^{-1}; Fig. 8) and the typical sediment accumulation rates at our stations are 0.015 g cm^{-2} yr^{-1} (Fig. 3). Accordingly, organic carbon is being buried into the deep sediments of Lake Superior at a rate of $\sim$ 0.7 mmol C m^{-2} d^{-1} ($\sim$ 3 g C m^{-2} yr^{-1}). The downward flux of carbon at the sediment–water interface (SWI) is due to both sediment accumulation and bioturbation:

$$F_{C\_SWI} = -D_b \left(\frac{dC}{dx}\right)_0 + \xi_0 U_0 C_0 \qquad (11)$$

For the bioturbation coefficient of 3 cm^2 yr^{-1}, the TOC concentration at the sediment surface of 4 wt%, and the organic carbon and porosity gradients shown in Fig. 8, these fluxes are on the order of 5–7 mmol m^{-2} d^{-1}. (This

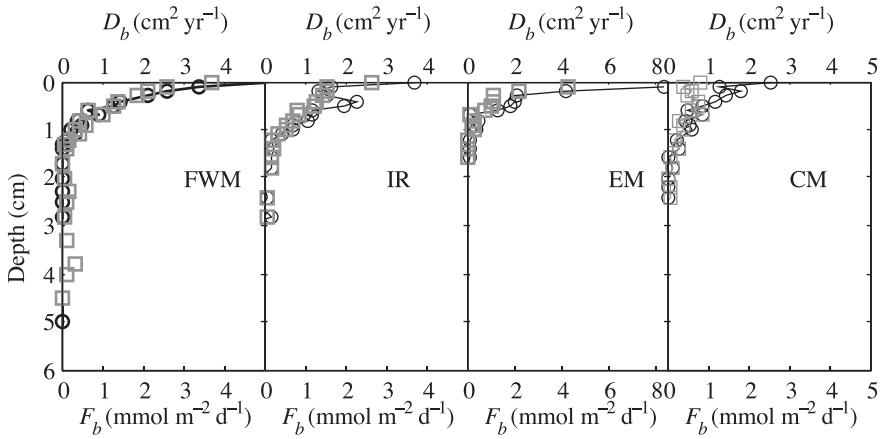

Fig. 10. Calculated bioturbation coefficients D_b (black circles) and the burial fluxes of organic carbon that are due to bioturbation, F_b (gray squares).

necessarily matches the downward oxygen fluxes [Table 2], as those were used to calculate the bioturbation coefficient.) Without the bioturbation flux, the burial flux alone accounts for only ~ 1.4 mmol C m^{-2} d^{-1} (~ 6 g C m^{-2} yr^{-1}).

The reactivity of organic matter in the surface sediment is high, with a characteristic time scale of degradation on the order of 1 yr (Table 2; Fig. 9), suggesting that the most labile organic fractions may decompose over a seasonal time scale. The reactivity decreases sharply within the top 2 cm, which is reflected in a much stronger decrease in the oxygen consumption rates (R_{O_2}), than in the organic carbon concentration (Fig. 9). The most reactive organic fractions are thus mineralized within the bioturbation zone and well above the depth of oxygen penetration. Below the bioturbation zone, the reactivity of organic carbon can be estimated by calculating the rate of organic carbon mineralization from the profile of TOC. At a steady state, by setting the left-hand side of Eq. 3 to zero and using $U\xi$ = const, one obtains:

$$R_C = -\xi U \frac{dC}{dx} \tag{12}$$

The reactivity k then can be calculated similarly to Eq. 10 as:

$$k = \frac{R_C}{\xi C} = -\frac{U}{C}\frac{dC}{dx} \tag{13}$$

For example, using the burial velocities, U, from Fig. 3 and the TOC concentrations, C, from Fig. 8, we obtain that the reactivity k below the depth of oxygen penetration at Sta. IR (4 cm) is on the order of 0.001 yr^{-1}.

Figure 11 illustrates the decrease in the reactivity of sediment organic matter, k, with age. In constructing this figure, the results for the reactivities calculated as a function of depth within the sediment (Fig. 9; Eqs. 7, 13) were combined with the relationship between the sediment depth and age shown in Fig. 3. In marine systems, the aging of organic material is often described by the Middelburg power law (Middelburg 1989; Middelburg et al. 1993), which holds over six orders of magnitude. Figure 11 shows that the reactivity of organic matter in the sediments of Lake Superior decreases with time after sediment deposition according to a similar power law. The reactivities calculated here for Lake Superior fall within the typical range of values observed in marine systems (Fig. 11). Given the low fraction (< 17%) of terrestrial organic material in these sediments (Zigah et al. 2011), this suggests that the relationships established for the decomposition of organic matter in marine environments may be transferable to the organic material produced in large freshwater lakes. The slope of the power-law line in Lake Superior, however, is steeper than the slope of the Middelburg line. The difference is statistically significant (at the two-sigma confidence level), suggesting that the degradation of organic material in Lake Superior occurs faster than in typical marine systems.

Sediment contribution to lake-wide carbon budget—The total oxygen uptake by Lake Superior sediments (Table 2) suggests a carbon degradation rate of 6.10 ± 1.39 mmol m^{-2} d^{-1}. Combined with the permanent burial flux of ~ 0.7 mmol C m^{-2} d^{-1}, this indicates that the total flux of organic carbon to the lake floor is about ~ 6.8 mmol m^{-2} d^{-1}. This is slightly higher but broadly consistent with previous estimates. The organic sedimentation flux was previously estimated in sediment traps in the Western arm of the lake at 2.3 mmol m^{-2} d^{-1} (Heinen and McManus 2004), in the central lake at 5–7.5 mmol m^{-2} d^{-1} (Baker et al. 1991; perhaps with a contribution from resuspended sediment), and in the Eastern basin at 2.5–3.5 mmol m^{-2} (Klump et al. 1989). Given the high reactivity of organic carbon (Table 2), the settling organic material may undergo substantial degradation while in sediment traps, and even poisoned traps are known to underestimate carbon amounts (Gardner 2000). Our estimates based on the total oxygen uptake therefore offer a complementary estimate.

The efficiency of sediment carbon mineralization is 6.1/6.8 = 90%, i.e., only 10% of the deposited organic carbon becomes buried into the deep sediments (below 15-cm depth). Such high efficiency is not unusual in aquatic sediments, but in marine environments it is more typical of hemipelagic and pelagic oceanic sediments (Reimers and Suess 1983) rather than sediments in ~ 200-m water depth.

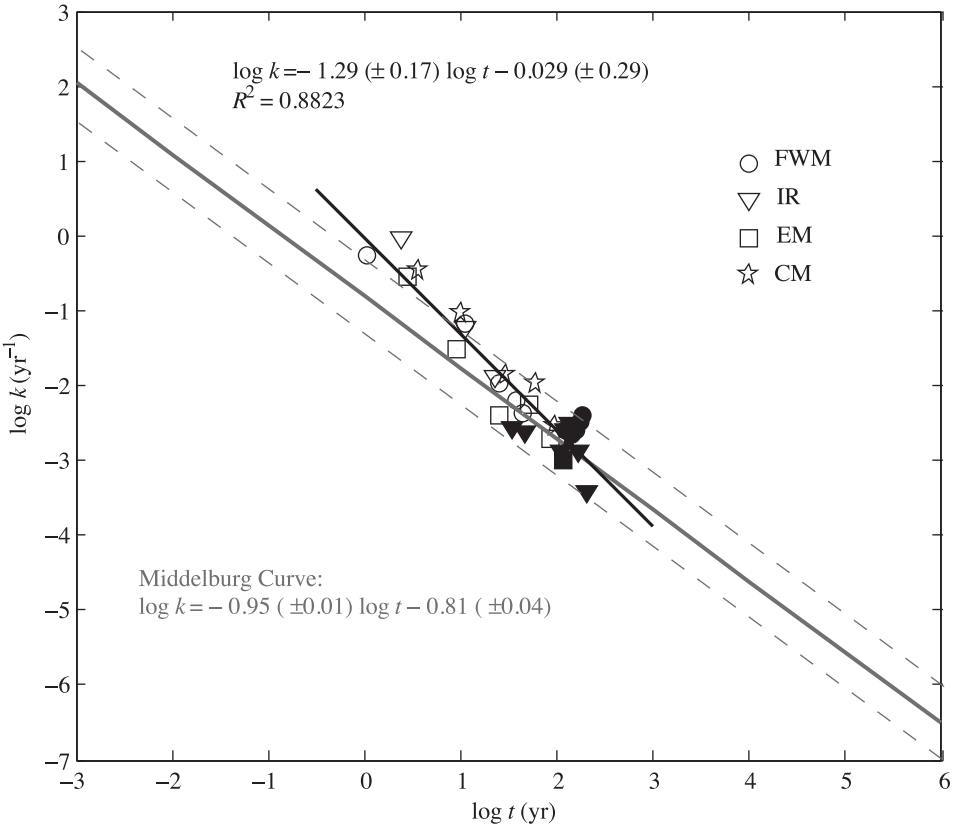

Fig. 11. Calculated reactivities of organic carbon as a function of the apparent sediment age, compared to Middelburg's model (gray line, Middelburg 1989) for the reactivity of organic matter in marine sediments. Open symbols correspond to the values of k calculated within the oxic zone using Eq. 7; filled symbols correspond to the values calculated in the sediment below oxygen penetration using Eq. 13. Dotted gray lines outline the typical range of values in marine sediments (Burdige 2007).

Assuming the average oxygen uptake of 6.10 ± 1.39 mmol m^{-2} d^{-1} as being representative of the Lake Superior sediments below 150 m, which underlie ~ 90% of the lake, the total rate of organic carbon mineralization in the deep basins of Lake Superior can be estimated at 1.65×10^{11} mol C yr^{-1} (or ~ 2 Tg yr^{-1}). This is ~ 20% of the carbon being produced by gross primary production, which was recently estimated based on measurements at selected locations at 9.7 Tg yr^{-1} (Sterner 2010). Given that large areas (about two-thirds) of the lake floor are non-depositional (do not retain fine-grained sediments; Kemp et al. 1978), the actual contribution of sediments to carbon mineralization is probably somewhat lower. The 20% number is close to values observed in similar water depths in marine environments (Suess 1980), but higher than a previous estimate for Lake Superior. The fraction of primary-produced organic carbon that reaches the sediments was previously estimated at 5%, based on the amount of carbon collected in open-water sediment traps (Baker et al. 1991). The burial flux into the deep sediments (0.24 Tg yr^{-1}, projected from our measurements for the entire lake) represents 2.5% of the estimated gross primary production, which agrees well with the typical range for deep temperate lakes (Alin and Johnson 2007).

Controls on oxygen penetration and carbon mineralization efficiency—The oxygen fluxes, 2–7 mmol m^{-2} d^{-1}, and the rates or carbon mineralization, ~ 1 μmol cm^{-3} d^{-1} (Fig. 6), in the upper sediment layer are similar to those found in marine sediments in similar water depths, ~ 200 m (Fig. 12; Sauter et al. 2001; Glud 2008). However, in coastal marine sediments, oxygen penetration rarely exceeds a few millimeters (Glud 2008; Mouret et al. 2010; Fig. 12), whereas in Lake Superior it is routinely below 3 cm (Figs. 5, 12). Sedimentation rate is a better predictor of sediment characteristics than water depth (Fig. 13). When plotted against the sedimentation rate (~ 0.02 g cm^{-2} yr^{-1}; ~ 0.03 cm yr^{-1}), both oxygen uptake and carbon burial efficiency match well the corresponding values in marine sediments, whereas the oxygen penetration depth is at the upper limit of the corresponding marine range. As most carbon mineralization in Lake Superior occurs in the upper few centimeters of sediment (Fig. 6), the low sedimentation rate translates to slow burial of organic material, allowing sufficient time for mineralization and a low oxygen demand in the deep sediment. In addition, several other factors, absent in marine sediments, contribute to the deep oxygen penetration in Lake Superior. The solubility of oxygen in freshwater is about 30% higher than in saltwater of the

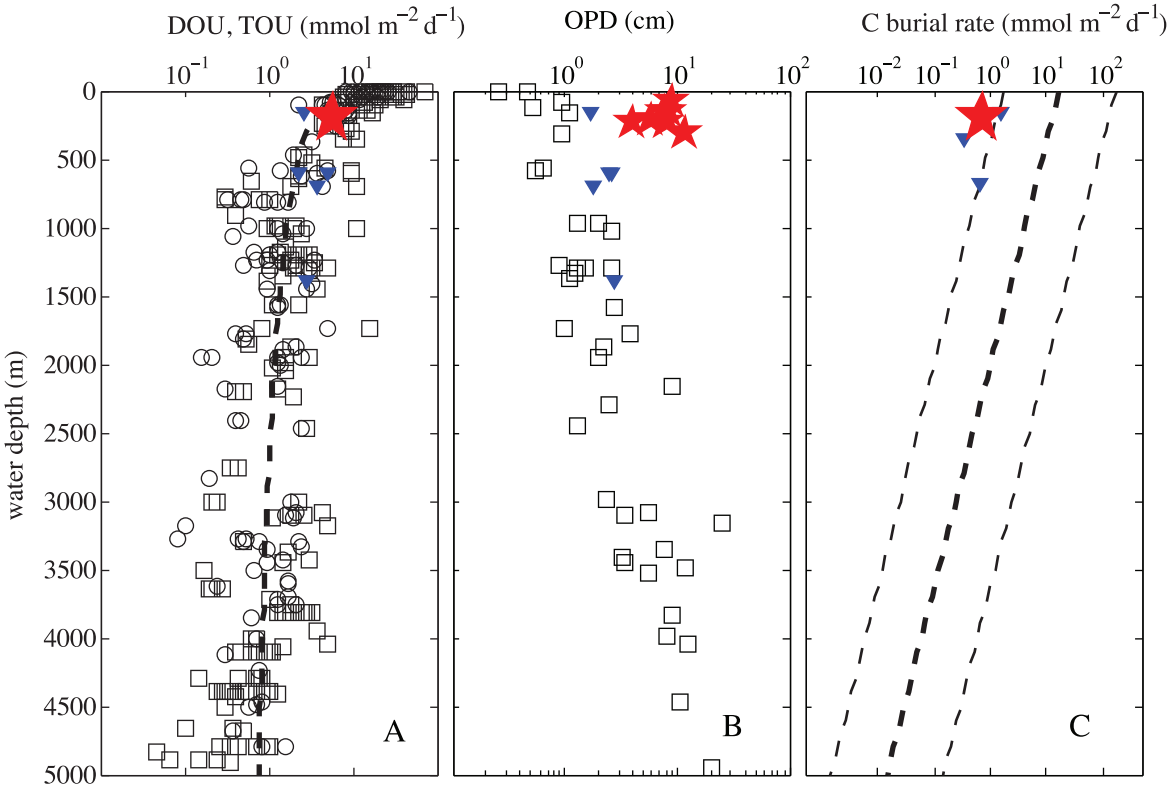

Fig. 12. Lake Superior sediments in comparison to other lacustrine and marine systems. Stars are results for Lake Superior from this study. Filled triangles are quantities derived using Lake Baikal data (Maerki et al. 2006, Müller et al. 2005) for comparison. (A) Diffusive oxygen uptake (DOU, circles) and total oxygen uptake (TOU, squares) in marine sediments (replotted from Glud 2008) and lake sediments (dotted line corresponds to the equation from den Heyer and Kalff 1998). (B) Oxygen penetration depth. Data points are for marine sediments, from Glud (2008). (C) Carbon burial rate. Lines correspond to the typical range in marine sediments, from Middelburg et al. (1997).

same temperature. The cold (3–5°C year-round) bottom waters of Lake Superior, renewed regularly by overturns, thus routinely carry more oxygen than oceanic bottom waters. In addition, compared to marine sediments where bioturbation extends to 10-cm depth or deeper (Boudreau 1998), the shallow bioturbation zone (~ 2 cm; Fig. 10) in Lake Superior leads to a less efficient transport of reactive organic material into the deep sediment, lowering the oxygen demand there. The longer exposure of organic matter to oxygen, however, seems to have little effect on the efficiency of carbon burndown (Fig. 13). Sediment resuspension, which contributes to low burial efficiency of marine organic carbon in muddy deltaic sediments (Fig. 13) (Canfield 1994; Aller et al. 2010), also seems to affect carbon mineralization insignificantly, despite the evidence for episodic resuspension of sediment by bottom currents (Zigah et al. 2011).

Non–steady-state diagenesis—Despite the spatial heterogeneity of Lake Superior sediments (Figs. 2, 8), our data set allows inferences about the temporal variability. Our results suggest that in Lake Superior the sediment depth of oxygen penetration experiences significant (by up to 2 cm) seasonal variations (Fig. 5). The OPD reflects the balance between the availability of oxygen from the bottom waters and the rate of oxygen consumption in the sediment. Numerical simulations of Katsev et al. (2006) demonstrated that the OPD is especially sensitive to this balance in deeply oxygenated sediments. The simulations also showed that in such sediments variations in bottom-water oxygen levels modify the OPD stronger, and on shorter time scales, than changes in the amount of settling organic matter. The reason is that, to affect the OPD, the reactive organic material needs to be transported into the deep sediment by burial or bioturbation. Our observations in Lake Superior support these predictions. Although the deposited organic matter is sufficiently reactive for some of its fractions to decompose on a seasonal time scale (Table 2) and carbon decomposition rates near the sediment surface appear to vary seasonally (Figs. 6, 7), the burial rates are slow (Fig. 3) and the bioturbation is shallow (Fig. 10). Accordingly, no significant correlation can be found between the fluxes of oxygen (Fig. 7) and the OPD. In contrast, that the shallowest oxygen penetration was observed at the end of winter stratification, when the oxygen levels in the bottom waters were at their lowest (~ 67% saturation at atmospheric pressure) (Figs. 4, 7), suggests that the seasonal variations in OPD are regulated by the oxygenation of the water column (Fig. 4). Changes in the bottom-water oxygen levels displace the OPD on the time scale of diffusion, $\tau = x^2/(2D_s)$; for example, diffusion to $x = 8$ cm takes ~ 2 months (for $D = 421$ cm^2 yr^{-1} used above). In

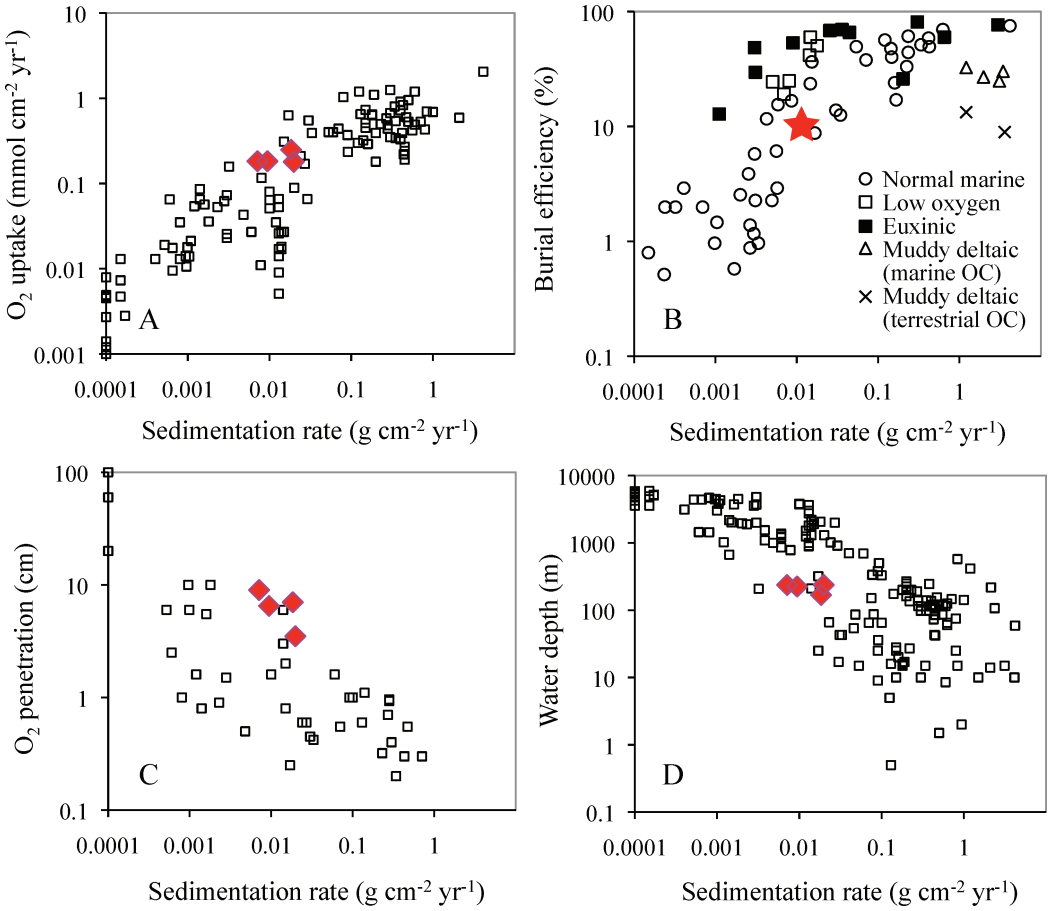

Fig. 13. Lake Superior sediments in comparison to marine sediments, plotted by sedimentation rate. Red symbols are the results for Lake Superior from this study. Marine sediment data are replotted from Canfield (1989, 1994) and Burdige (2007). (A) Total oxygen uptake. (B) Burial efficiency relative to carbon sedimentation flux. The star marks the values averaged over sampled stations. (C) Oxygen penetration depth. (D) Water column depth.

Lake Superior, therefore, the OPD should respond with time lags ranging from several weeks (for shallower OPDs, e.g., Sta. IR) to several months (for deeper OPDs, e.g., Sta. CM and ED). At stations with deep OPDs, the oxygenation of the water column in June (Fig. 4) therefore would result in a deepening OPD in mid- to late summer, consistent with our observations (Fig. 5).

Organic C sedimentation may modify the OPD on decadal and longer time scales. These may be long enough for the positions of the redox boundary to become marked by the accumulation of Fe and Mn (Katsev et al. 2006), such as in Fig. 2. The trends in organic sedimentation in Lake Superior are unclear, as the historical data on primary productivity are scarce. If we assume that the organic sedimentation in Lake Superior followed the availability of phosphorus, the limiting nutrient (Nalewajko et al. 1981; Sterner et al. 2004), then the sedimentation flux of organic carbon probably doubled between the beginning of the 20th century and the mid-1970s and then declined in the 1990s (Lesht et al. 1991). This would result in a temporary shallowing of the redox boundary and the accumulation of Fe and Mn at shallower depths. These layers could now be located within the presently oxic sediment, in violation of the steady-state redox sequence. Given the strong lateral heterogeneity of the sediments (Fig. 2), however, this hypothesis is difficult to test. It is possible that local redox changes over a variety of time scales could be caused by physical disturbances. For instance, bottom currents (Bennington et al. 2010) may episodically remove (or deposit) the organic-rich upper sediment layer, thereby exposing (or covering) the underlying organic-poor sediment.

The observed centimeter-scale migrations in oxygen penetration depth suggest that temporal redox variability in deeply oxygenated sediments may be greater than previously acknowledged. These changes may lead, in particular, to the variability in the transformations of other redox-sensitive elements, such as nitrogen. Nitrogen cycling is of particular interest in Lake Superior because of the buildup of nitrate in the water column and an exceptionally high N : P ratio (Sterner et al. 2007; Sterner 2011). That sediment OPD responds to the oxygen supply from the bottom waters suggests that sediment redox chemistry may be affected by the physical stratification of the water column, which is now being affected by climate warming (Austin and Colman 2008). Given the similarity to marine hemipelagic sediments (Fig. 13), analogous processes could be expected in oceanic sediments in response to changing ocean ventilation, such as during oceanic anoxia events.

Acknowledgments

We thank Jay Austin for sharing his National Science Foundation (NSF)–funded cruise opportunities in June and October 2009. Jay Austin, Elizabeth Minor, and Robert Sterner are acknowledged for sharing their water column temperature and oxygen data obtained under NSF Ocean Sciences (OCE) grants 0825633, 0927512, and 0825600, Ronnie Glud for sharing his data compilation on oxygen penetrations and consumption rates, and Elizabeth Minor and Josef Werne for sharing their laboratory facilities. For intellectual contributions, we are particularly thankful to Thomas C. Johnson, Robert Sterner, Jacques Finlay, Jim Cotner, Robert Hecky, Stephanie Guildford, Elizabeth Minor, and Maria Dittrich. We thank captain Mike King and the crew of R/V *Blue Heron*, marine technician Jason Agnich, and laboratory technician Sarah Grosshuesch. ^{210}Pb data for the Isle Royale (IR) and Far Western Mooring (FWM) stations were provided by Amy Kireta and Euan Reavie (Natural Resources Research Institute, University of Minnesota Duluth), supported by Minnesota Sea Grant. Sediment cores were split and logged at the Limnological Research Center, Department of Geology and Geophysics, University of Minnesota–Twin Cities with the help of Anders Noren and Kristina Brady. The work has been supported by the NSF OCE 0961720 grant and the University of Minnesota Duluth start-up funds to S.K., Water Resources Science Block Grant to J.L., University of Minnesota Duluth Physics Department summer fellowships to J.L. and D.M., and Undergraduate Research Opportunities Program to D.M. We thank two anonymous reviewers for comments that helped improve the manuscript.

References

Alin, S., and T. C. Johnson. 2007. Carbon cycling in large lakes of the world: A synthesis of production, burial, and lake–atmosphere exchange estimates. Global Biogeochem. Cycles **21:** GB3002, doi:10.1029/2006GB002881

Aller, R. C., V. Madrid, A. Chistoserdov, J. Y. Aller, and C. Heilbrun. 2010. Unsteady diagenetic processes and sulfur biogeochemistry in tropical deltaic muds: Implications for oceanic isotopic cycles and the sedimentary record. Geochim. Cosmochim. Acta **74:** 4671–4692, doi:10.1016/j.gca.2010.05.008

Appleby, P. G., and F. Oldfield. 1978. The calculation of lead-210 dates assuming a constant rate of supply of unsupported ^{210}Pb to the sediment. Catena **5:** 1–8, doi:10.1016/S0341-8162(78)80002-2

Austin, J., and S. Colman. 2008. A century of temperature variability in Lake Superior. Limnol. Oceanogr. **53:** 2724–2730, doi:10.4319/lo.2008.53.6.2724

Baker, J. E., S. J. Eisenreich, and B. J. Eadie. 1991. Sediment trap fluxes and benthic recycling of organic carbon, polycyclic aromatic hydrocarbons, and polychlorobiphenyl congeners in Lake Superior. Environ. Sci. Technol. **25:** 500–509, doi:10.1021/es00015a019

Bennington, V., G. A. McKinley, N. Kimura, and C. H. Wu. 2010. General circulation of Lake Superior: Mean, variability, and trends from 1979 to 2006. J. Geophys. Res **115:** C12015, doi:10.1029/2010JC006261

Berner, R. A. 1980. Early diagenesis: A theoretical approach. Princeton Univ. Press.

Boudreau, B. P. 1997. Diagenetic models and their implementation: Modeling transport and reactions in aquatic sediments. Springer.

———. 1998. Mean mixed depth of sediments: The wherefore and the why. Limnol. Oceanogr. **43:** 524–526, doi:10.4319/lo.1998.43.3.0524

Burdige, D. J. 2007. Preservation of organic matter in marine sediments: controls, mechanisms, and an imbalance in sediment organic carbon budgets? Chem. Rev. **107:** 467–485, doi:10.1021/cr050347q

Canfield, D. E. 1989. Sulfate reduction and oxic respiration in marine sediments: Implications for organic carbon preservation in euxinic environments. Deep-Sea Res. **36:** 121–138.

———. 1994. Factors influencing organic carbon preservation in marine sediments. Chem. Geol. **114:** 315–329, doi:10.1016/0009-2541(94)90061-2

———, and others. 1993. Pathways of organic carbon oxidation in three continental margin sediments. Mar. Geol. **113:** 27–40, doi:10.1016/0025-3227(93)90147-N

Carlton, R. G., G. S. Walker, M. J. Klug, and R. G. Wetzel. 1989. Relative values of oxygen, nitrate, and sulfate to terminal microbial processes in the sediments of Lake Superior. J. Great Lakes Res. **15:** 133–140, doi:10.1016/S0380-1330(89)71467-2

Cole, J. J., and others. 2007. Plumbing the global carbon cycle: Integrating inland waters into the terrestrial carbon budget. Ecosystems **10:** 171–184, doi:10.1007/s10021-006-9013-8

Cotner, J. B., B. A. Biddanda, W. Makino, and E. Stets. 2004. Organic carbon biogeochemistry of Lake Superior. Aquat. Ecosyst. Health Manage. **7:** 451–464, doi:10.1080/14634980490513292

den Heyer, C., and J. Kalff. 1998. Organic matter mineralization rates in sediments: A within- and among-lake study. Limnol. Oceanogr. **43:** 695–705, doi:10.4319/lo.1998.43.4.0695

Evans, J. E., T. C. Johnson, E. C. Alexander, Jr, R. S. Lively, and S. J. Eisenreich. 1981. Sedimentation rates and depositional processes in Lake Superior from ^{210}Pb geochronology. J. Great Lakes Res. **7:** 299–310, doi:10.1016/S0380-1330(81)72058-6

Gardner, W. D. 2000. Sediment trap sampling in surface waters, p. 240–281. *In* R. B. Hanson, H. W. Ducklow, and J. G. Field [eds.], The changing ocean carbon cycle: A midterm synthesis of the Joint Global Ocean Flux Study. Cambridge Univ. Press.

Gehlen, M., C. Rabouille, U. Ezat, and L. D. Guidi-Guilvard. 1997. Drastic changes in deep-sea sediment porewater composition induced by episodic input of organic matter. Limnol. Oceanogr. **42:** 980–986, doi:10.4319/lo.1997.42.5.0980

Glud, R. N. 2008. Oxygen dynamics of marine sediments. Mar. Biol. Res. **4:** 243–289, doi:10.1080/17451000801888726

Gobeil, C., B. Sundby, R. W. Macdonald, and J. N. Smith. 2001. Recent change in organic carbon flux to Arctic Ocean deep basins: Evidence from acid volatile sulfide, manganese and rhenium discord in sediments. Geophys. Res. Lett. **28:** 1743–1746, doi:10.1029/2000GL012491

Gudasz, C., D. Bastviken, K. Steger, K. Premke, S. Sobek, and L. J. Tranvik. 2010. Temperature-controlled organic carbon mineralization in lake sediments. Nature **466:** 478–481, doi:10.1038/nature09186

Heinen, E. A., and J. McManus. 2004. Carbon and nutrient cycling at the sediment–water boundary in Western Lake Superior. J. Great Lakes Res. **30:** 113–132, doi:10.1016/S0380-1330(04)70381-0

Johnson, T. C., J. E. Evans, and S. J. Eisenreich. 1982. Total organic carbon in Lake Superior sediments: Comparisons with hemipelagic and pelagic marine environments. Limnol. Oceanogr. **27:** 481–491, doi:10.4319/lo.1982.27.3.0481

Jørgensen, B. B. 1982. Mineralization of organic matter in the sea bed—the role of sulphate reduction. Nature **296:** 643–645, doi:10.1038/296643a0

Katsev, S., G. Chaillou, B. Sundby, and A. Mucci. 2007. Effects of progressive oxygen depletion on sediment diagenesis and fluxes: A model for the low St. Lawrence River Estuary. Limnol. Oceanogr. **52:** 2555–2568, doi:10.4319/lo.2007.52.6.2555

———, B. Sundby, and A. Mucci. 2006. Modeling vertical excursions of the redox boundary in sediments: Application to deep basins of the Arctic Ocean. Limnol. Oceanogr. **51:** 1581–1593, doi:10.4319/lo.2006.51.4.1581

Kemp, A. L. W., C. I. Dell, and N. S. Harper. 1978. Sedimentation rates and a sediment budget for Lake Superior. J. Great Lakes Res. **4:** 276–287, doi:10.1016/S0380-1330(78)72198-2

Klump, J. V., R. Paddock, C. C. Remsen, S. Fitsgerald, M. Boraas, and P. Anderson. 1989. Variation in accumulation rates and the flux of labile organic matter in eastern Lake Superior basins. J. Great Lakes Res. **15:** 104–122, doi:10.1016/S0380-1330(89)71465-9

Lesht, B. M., T. D. Fontaine, III, and D. M. Dolan. 1991. Great Lakes total phosphorus model: Post audit and regionalized sensitivity analysis. J. Great Lakes Res. **17:** 3–17, doi:10.1016/S0380-1330(91)71337-3

Li, J. 2011. Diagenesis and sediment-water exchanges in organic-poor sediments of Lake Superior. M.Sc. thesis. Univ. of Minnesota.

Lorke, A., B. Muller, M. Maerki, and A. Wüest. 2003. Breathing sediments: The control of diffusive transport across the sediment–water interface by periodic boundary-layer turbulence. Limnol. Oceanogr. **48:** 2077–2085, doi:10.4319/lo.2003.48.6.2077

Maerki, M., B. Müller, and B. Wehrli. 2006. Microscale mineralization pathways in surface sediments: A chemical sensor study in Lake Baikal. Limnol. Oceanogr. **51:** 1342–1354, doi:10.4319/lo.2006.51.3.1342

Matisoff, G., and X. Wang. 1998. Solute transport in sediments by freshwater infaunal bioirrigators. Limnol. Oceanogr. **43:** 1487–1499, doi:10.4319/lo.1998.43.7.1487

McManus, J., E. A. Heinen, and M. M. Baehr. 2003. Hypolimnetic oxidation rates in Lake Superior: Role of dissolved organic material on the lake's carbon budget. Limnol. Oceanogr. **48:** 1624–1632, doi:10.4319/lo.2003.48.4.1624

Meile, C., and P. Van Cappellen. 2003. Global estimates of enhanced solute transport in marine sediments. Limnol. Oceanogr. **48:** 777–786, doi:10.4319/lo.2003.48.2.0777

Meysman, F. J. R., B. P. Boudreau, and J. J. Middelburg. 2005. Modeling reactive transport in sediments subject to bioturbation and compaction. Geochim. Cosmochim. Acta **69:** 3601–3617, doi:10.1016/j.gca.2005.01.004

Middelburg, J. J. 1989. A simple rate model for organic matter decomposition in marine sediments. Geochim. Cosmochim. Acta **53:** 1577–1581, doi:10.1016/0016-7037(89)90239-1

———, K. Soetaert, and P. M. J. Herman. 1997. Empirical relationships for use in global diagenetic models. Deep-Sea Res. I **44:** 327–344.

———, T. Vlug, F. Jaco, and W. A. van der Nat. 1993. Organic matter mineralization in marine systems. Global Planet. Change **8:** 47–58.

Mouret, A., and others. 2010. Oxygen and organic carbon fluxes in sediments of the Bay of Biscay. Deep-Sea Res. I **57:** 528–540.

Müller, B., M. Maerki, M. Schmid, E. G. Vologina, B. Wehrli, A. Wüest, and M. Sturm. 2005. Internal carbon and nutrient cycling in Lake Baikal: Sedimentation, upwelling, and early diagenesis. Global Planet. Change **46:** 101–124.

Munawar, M., and I. F. Munawar. 1978. Phytoplankton of Lake Superior 1973. J. Great Lakes Res. **4:** 415–442, doi:10.1016/S0380-1330(78)72212-4

Nalewajko, C., K. Lee, and H. Shear. 1981. Phosphorus kinetics in Lake Superior: Light intensity and phosphate uptake in algae. Can. J. Fish. Aquat. Sci. **38:** 224–232, doi:10.1139/f81-029

Ostrom, N. E., D. T. Long, E. M. Bell, and T. Beals. 1998. The origin and cycling of particulate and sedimentary organic matter and nitrate in Lake Superior. Chem. Geol. **152:** 12–28.

Reimers, C. E., and E. Suess. 1983. The partitioning of organic carbon fluxes and sedimentary organic matter decomposition rates in the ocean. Mar. Chem. **13:** 141–168, doi:10.1016/0304-4203(83)90022-1

Revsbech, N. P. 1989. An oxygen microelectrode with a guard cathode. Limnol. Oceanogr. **34:** 472–476, doi:10.4319/lo.1989.34.2.0474

Sauter, E. J., M. Schluter, and E. Suess. 2001. Organic carbon flux and remineralization in surface sediments from the northern North Atlantic derived from pore-water oxygen microprofiles. Deep-Sea Res. I **48:** 529–553.

Sayles, F. L., W. R. Martin, and W. G. Deuser. 1994. Response of benthic oxygen-demand to particulate organic-carbon supply in the deep-sea near Bermuda. Nature **371:** 686–689, doi:10.1038/371686a0

Sobek, S., E. Durisch-Kaiser, R. Zurbrügg, N. Wongfun, M. Wessels, N. Pasche, and B. Wehrli. 2009. Organic carbon burial efficiency in lake sediments controlled by oxygen exposure time and sediment source. Limnol. Oceanogr. **54:** 2243–2254, doi:10.4319/lo.2009.54.6.2243

Sterner, R. W. 2010. In situ-measured primary production in Lake Superior. J. Great Lakes Res. **36:** 139–149, doi:10.1016/j.jglr.2009.12.007

———. 2011. C:N:P stoichiometry in Lake Superior: freshwater sea as end member. Inland Waters **1:** 29–46.

———, T. M. Smutka, R. M. L. McKay, X. Qin, E. T. Brown, and R. M. Sherrell. 2004. Phosphorus and trace metal limitation of algae and bacteria in Lake Superior. Limnol. Oceanogr. **49:** 495–507, doi:10.4319/lo.2004.49.2.0495

———, and others. 2007. Increasing stoichiometric imbalance in North America's largest lake: Nitrification in Lake Superior. Geophys. Res. Lett. **34:** L10406, doi:10.1029/2006GL028861

Suess, E. 1980. Particulate organic carbon flux in the oceans: Surface productivity and oxygen utilization. Nature **288:** 260–263, doi:10.1038/288260a0

Sweerts, J.-P. R. A., C. A. Kelly, J. W. M. Rudd, R. Hesslein, and T. E. Cappenberg. 1991. Similarity of whole-sediment molecular diffusion coefficients in freshwater sediments of low and high porosity. Limnol. Oceanogr. **36:** 335–342, doi:10.4319/lo.1991.36.2.0335

Thomsen, U., B. Thumdrup, D. A. Stahl, and D. E. Canfield. 2004. Pathways of organic carbon oxidation in a deep lacustrine sediment, Lake Michigan. Limnol. Oceanogr. **49:** 2046–2057, doi:10.4319/lo.2004.49.6.2046

Tranvik, L. J., and others. 2009. Lakes and impoundments as regulators of carbon cycling and climate. Limnol. Oceanogr. **54:** 2298–2314, doi:10.4319/lo.2009.54.6_part_2.2298

van Alstine, J. D. 2006. A high resolution study of the spatial and temporal variability of natural and anthropogenic compounds in offshore Lake Superior sediments. M.Sc. thesis. Univ. of Minnesota.

Zigah, P. K., E. C. Minor, J. P. Werne, and L. McCallister. 2011. Radiocarbon and stable carbon isotope insights into provenance and cycling of carbon in Lake Superior. Limnol. Oceanogr. **56:** 867–886, doi:10.4319/lo.2011.56.3.0867

Associate editor: Ronnie Nøhr Glud

Received: 19 December 2011
Accepted: 22 May 2012
Amended: 22 June 2012